[2]G. D. Wignall and P. A. Egelstaff, J. Phys. C **1**, 1088 (1968).
[3]P. D. Adams, Phys. Rev. Lett. **25**, 1012 (1970).
[4]H. K. Schürman and R. D. Parks, Phys. Rev. Lett. **26**, 367 (1971); Phys. Rev. Lett. **26**, 835 (1971).
[5]H. K. Schürman and R. D. Parks, Phys. Rev. Lett. **27**, 1790 (1971).
[6]H. K. Schürman and R. D. Parks, Phys. Rev. B **6**, 348 (1972).
[7]D. Stroud, Phys. Rev. B **7**, 4405 (1973).
[8]S. Tamaki, Phys. Lett. A **40**, 17 (1972).
[9]J. K. Percus and G. J. Yevick, Phys. Rev. **110**, 1 (1958).
[10]J. A. Lebowitz and J. S. Rowlinson, J. Chem. Phys. **41**, 133 (1964).
[11]T. Schneider, R. Brout, H. Thomas, and J. Feder, Phys. Rev. Lett. **25**, 1423 (1970).
[12]See, for example, L. D. Landau and I. M. Lifschitz, *Statistical Physics* (Pergamon, London, 1958), pp. 401 and 402.
[13]See, for example, L. P. Kadanoff, and G. Baym, *Quantum Statistical Mechanics* (Benjamin, New York, 1962).
[14]See, for example, R. Brout, *Phase Transitions* (Benjamin, New York, 1965).
[15]See, for example, W. A. Harrison, *Pseudopotentials in the Theory of Metals* (Benjamin, New York, 1966).
[16]N. W. Ashcroft, Phys. Lett. **23**, 48 (1966).
[17]V. Heine and I. Abarenkov, Philos. Mag. **9**, 451 (1964). The potentials, as calculated by V. Heine and A. O. E. Animalu [Philos. Mag. **12**, 1249 (1965)] are conveniently tabulated in Ref. 15.
[18]J. Hubbard, Proc. R. Soc. A **243**, 336 (1957).
[19]N. W. Ashcroft and D. C. Langreth, Phys. Rev. **159**, 500 (1967).
[20]See, for example, D. Pines and P. Nozières, *The Theory of Quantum Liquids* (Benjamin, New York, 1966), Vol. I.
[21]M. E. Fisher and J. S. Langer, Phys. Rev. Lett. **20**, 665 (1968).
[22]N. W. Ashcroft and D. C. Langreth, Phys. Rev. **155**, 682 (1967).

PHYSICAL REVIEW B VOLUME 8, NUMBER 4 15 AUGUST 1973

Anharmonic Contributions to Elastic and Inelastic Scattering of X Rays at Bragg Reflections in Aluminum

G. Albanese
Istituto di Fisica dell'Università, Parma, Italy
and Gruppo Nazionale di Struttura della Materia, Consiglio Nazionale delle Ricerche, Italy

C. Ghezzi
Laboratorio MASPEC del Consiglio Nazionale delle Ricerche, Parma, Italy
and Gruppo Nazionale di Struttura della Materia, Consiglio Nazionale delle Ricerche, Italy

(Received 4 December 1972)

The scattering intensities of the 14.4-KeV γ rays from Co^{57} were measured at the {333} and {444} reflections of Al crystals in the temperature range 295-800 °K. The elastic and inelastic components of the scattered intensities were separated by means of the Mössbauer effect. The temperature dependences of the integrated intensities of the elastic peaks give evidence of non-Gaussian anharmonic contributions to the Debye–Waller factors. Comparison is also made between experimental and calculated temperature dependences of the inelastic intensities. Some of the discrepancies found at the {444} reflection are explained by admitting a non-neglectable contribution of non-Gaussian terms in the correlation part of the formula for the intensity of the thermal diffuse scattering.

I. INTRODUCTION

As is known, the thermal motion of the atoms in a crystal lattice causes a weakening of the Bragg diffraction lines and an increase in the total amount of the thermal diffuse scattering (TDS). Thus, in principle, x-ray-diffraction experiments can give information about the dynamics of the lattice. For example, the mean-square vibration amplitude of the atoms can be obtained from the temperature dependence of the integrated intensities of Bragg peaks, whereas by measuring the TDS intensity at different sites in the Brillouin zone one can obtain the dispersion curves of the lattice phonons.[1] The greatest part of experimental research in this field is mainly related to the atomic motion as described in the harmonic approximation.

The suggestion that diffraction experiments would also be useful to give evidence of anharmonic effects was first given by Waller.[2] Since then a lot of theoretical and experimental investigations have been performed, especially regarding the anharmonic contributions to the Debye-Waller factor. However, in order to separate anharmonic effects it is often necessary to make experiments at high-order reflections and at elevated temperatures. In these experimental conditions the intensity scattered at a reciprocal-lattice node is quite appreciably made up of those x-ray photons which suffer inelastic scattering by the thermal vibrations of the lattice. Both elastic and inelastic scatterings are affected by anharmonic interactions. However, it is necessary to separate them in order to obtain substantiated information on the amount of anharmonic contributions.

The only way to accurately separate the TDS from the crystalline reflections is to use the high-energy resolution of the Mössbauer effect. This

method was described and discussed in two previous papers,[3,4] where the 14.4-keV ($\lambda = 0.8602$ Å) Mössbauer radiation emitted by the Fe^{57} nuclide was used to investigate the intensity of TDS at the Bragg peaks as a function of temperature and of the order of reflection in Si crystals. We found that the angular and temperature dependence of the TDS intensity was that of the one-phonon scattering term. The higher-order terms did not give any appreciable contribution because of the high Debye temperature (543 °K) of Si. Subsequently[5] we applied the Mössbauer effect to study the temperature dependence of TDS at the {800} and {1000} Bragg reflections of KCl. Owing to the high order of the above reflections and the relatively low value of the Debye temperature of KCl (230 °K), we were able to show at high temperatures important contributions to the TDS by multiphonon scattering processes. Anharmonic effects were found to be quite negligible in Si, whereas in KCl it was enough to account for the effect of thermal expansion on the lattice frequencies in order to fit the experimental temperature dependences of both elastic and inelastic intensities with the calculated ones.

In this paper we describe the observation of large anharmonic contributions to the Debye–Waller factor and to the TDS intensity in aluminum crystals at elevated temperatures. These observations were made by using the Mössbauer effect to measure the temperature dependence of both elastic and inelastic intensities at the {333} and {444} Bragg reflections. The observed anharmonic contributions are shown to be much larger than those predicted by taking account only of the thermal expansion of the lattice and the result is shown to be made up appreciably by non-Gaussian terms.

II. THEORY

The theory of the effect of thermal vibrations on x-ray scattering, when anharmonic effects are taken into account, has been approached by a number of authors.[6–11] In this section, those general features which are directly related to the present experiment are briefly summarized.

The intensity of scattering of x-rays from a crystal of identical atoms with scattering factor f is given in electron units by

$$I(\vec{Q}) = f^2 \sum_{ll'} e^{i\vec{Q}\cdot(\vec{R}_l - \vec{R}_{l'})} \langle e^{i\vec{Q}\cdot(\vec{u}_l - \vec{u}_{l'})} \rangle , \tag{1}$$

where $\vec{Q}$ is the scattering vector, that is, the difference between the wave vectors $\vec{k}$ and $\vec{k}_0$ of scattered and incident x rays, respectively. $\vec{R}_l$ and $\vec{u}_l$ are vectors indicating the equilibrium position and the displacement of atom l, respectively. The brackets denote thermal average.

Elastic Scattering

The Debye–Waller factor is related to the intensity for Bragg scattering and is given by those terms in (1) which are independent of both l and l'. Thus, the effect of the thermal motion on the elastic intensity is equivalent to multiplying the scattering factor of each atom by the temperature factor

$$e^{-M} = \langle e^{i\vec{Q}\cdot\vec{u}_l} \rangle . \tag{2}$$

If the equilibrium position of the atoms is centrosymmetric and if the displacements $\vec{u}_l$ are small or if they follow a Gaussian distribution, we have exactly[1]

$$e^{-M} = \langle e^{i\vec{Q}\cdot\vec{u}_l} \rangle = e^{-\langle(\vec{Q}\cdot\vec{u}_l)^2\rangle/2} = e^{-Q^2\langle u_{lQ}^2\rangle/2} , \tag{3}$$

where u_{lQ} is the component of atomic displacement along the direction of the scattering vector $\vec{Q}$.

When the atomic displacements deviate from a Gaussian distribution, the result is[11]

$$\langle e^{i\vec{Q}\cdot\vec{u}_l} \rangle = \exp\{ -\tfrac{1}{2}\langle(\vec{Q}\cdot\vec{u}_l)^2\rangle + \tfrac{1}{24} [\langle(\vec{Q}\cdot\vec{u}_l)^4\rangle - 3\langle(\vec{Q}\cdot\vec{u}_l)^2\rangle^2] + O(Q^6)\} . \tag{4}$$

In the harmonic approximation the displacements $\vec{u}_l$ are small and have a Gaussian distribution. By assuming the Debye model for the lattice frequencies, we have from formula (3), in the high-temperature limit,

$$M = \frac{3\hbar^2 Q^2 T}{2mK_B\Theta^2} , \tag{5}$$

where Θ is the Debye temperature, m is the mass of the atom, and $\hbar$ and K_B are the Planck constant divided by 2π and the Boltzmann constant, respectively. Formula (5) is useful since it permits one to summarize the results of experiments on the Debye–Waller factor by means of the value of Θ.

When anharmonic interactions do not cause the atomic displacements to deviate appreciably from a Gaussian distribution, M contains additional terms which are proportional to T^2 (for example, the thermal expansion corrections), but it is still proportional to Q^2. Therefore expression (5) can still be applied to summarize experimental results by assuming that the Debye temperature Θ is a suitable function of the temperature of the crystal. For non-Gaussian distributions, however, this last procedure can no longer be applied, owing to the presence of the so-called anomalous term in Q^4 in the expression of M; this implies that different functions $\Theta = \Theta(T)$ should be assumed for different Q in order to fit experimental data by means of expression (5).

Inelastic Scattering

For a Gaussian distribution of atomic displacements the function $I(\vec{Q})$, which gives the intensity

of the total scattering at the point $\vec{Q}$, becomes

$$I(\vec{Q}) = f^2 e^{-2M} \sum_{ll'} e^{i\vec{Q}\cdot(\vec{R}_l - \vec{R}_{l'})} e^{Q^2\langle u_{lQ} u_{l'Q}\rangle}$$

$$= f^2 e^{-2M} \left(\sum_{ll'} e^{i\vec{Q}\cdot(\vec{R}_l - \vec{R}_{l'})} + \sum_{ll'} e^{i\vec{Q}\cdot(\vec{R}_l - \vec{R}_{l'})} \times (e^{Q^2\langle u_{lQ} u_{l'Q}\rangle} - 1) \right), \quad (6)$$

with e^{-M} denoted by expression (3). The first summation, which differs from zero only when $\vec{Q}$ coincides with a reciprocal-lattice vector, gives Bragg scattering; the second one is related to the thermal diffuse scattering and can be written as

$$I_{TDS}(\vec{Q}) = Nf^2(1 - e^{-2M}) + f^2 e^{-2M} \times \sum_{l \neq l'} e^{i\vec{Q}\cdot(\vec{R}_l - \vec{R}_{l'})} (e^{Q^2\langle u_{lQ} u_{l'Q}\rangle} - 1)$$

$$= I_{Ein} + I_{corr}, \quad (7)$$

where N is the total number of atoms in the crystal. For the model of independent vibrations the average $\langle u_{lQ} u_{l'Q}\rangle$ vanishes if $l \neq l'$. Therefore, the two terms in expression (7) are called the Einstein and correlation terms, respectively. The first term I_{Ein} is a smooth function of the scattering angle, whereas I_{corr} gives broad peaks at the Bragg angles.

For non-Gaussian distributions one readily obtains

$$I_{TDS}(\vec{Q}) = Nf^2(1 - e^{-2M}) + f^2 e^{-2M} \sum_{l \neq l'} e^{i\vec{Q}\cdot(\vec{R}_l - \vec{R}_{l'})} \times (e^{Q^2\langle u_{lQ} u_{l'Q}\rangle + Q^4 \mathfrak{F}} - 1), \quad (8)$$

where now e^{-M} is given by expression (4), and

$$\mathfrak{F} = \tfrac{1}{12} [3\langle u_{lQ}^2 u_{l'Q}^2\rangle - 4\langle u_{lQ}^3 u_{l'Q}\rangle - 3(\langle u_{lQ}^2\rangle \langle u_{l'Q}^2\rangle - 4\langle u_{lQ} u_{l'Q}\rangle \langle u_{lQ}^2\rangle + 2\langle u_{lQ} u_{l'Q}\rangle^2)], \quad (9)$$

where terms in $O(Q^6)$ are neglected.

It must be rememebered that the TDS intensity integrated over an entire Brillouin zone (BZ) does not depend on the choice of the model for the lattice vibrations; in fact, the integral of the total scattered intensity (Bragg plus diffuse scattering) over a BZ is not affected by the displacements of the atoms from their equilibrium position.[12] It follows that the integral over a BZ of both correlation terms appearing in (7) and (8) is zero. This result suggests that the correlation terms give positive and negative contributions as $\vec{Q}$ is made to vary inside a BZ so that the TDS intensity is peaked at reciprocal-lattice nodes.

III. EXPERIMENTAL METHOD

The separation of the γ rays which are elastically scattered by the crystal from those which undergo inelastic scattering was done by using the same procedure described in previous papers.[3,4] A 50-mCi Co^{57} source diffused in a chromium matrix (10 mm high × 5 mm wide) was used together with a 310-stainless-steel absorber 98% enriched in Fe^{57}, with a thickness equal to 1 mg/cm^2 of Fe^{57}.

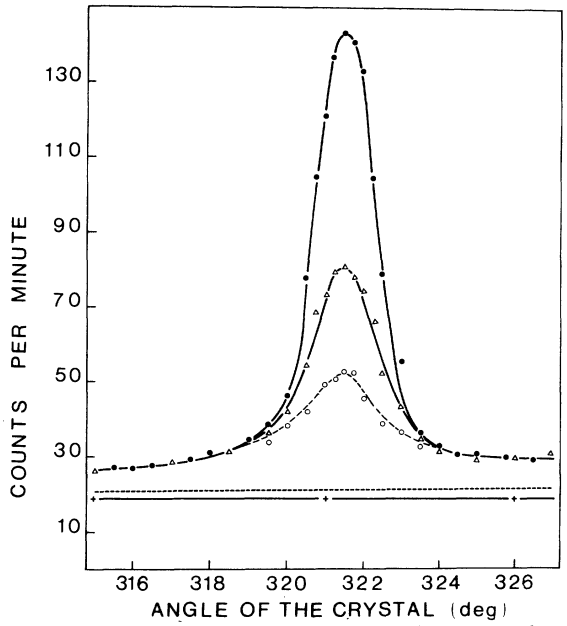

FIG. 1. Scattered intensities vs the glancing angle between incident beam and the surface of an Al crystal, {444} reflection, Bragg geometry, at room temperature. Closed circles and open triangles are experimental points and correspond to the curve of I_∞ and I_R (Mössbauer absorber out of and in resonance, respectively). Open circles were obtained from the two above sets of experimental data and correspond to the curve (dashed) of the inelastic intensity. The straight line under the curve is the hard γ and cosmic background. The dashed straight line is the calculated Compton scattering.

The Al crystals were rectangular lamellas (15×15 mm^2), about 2 mm thick, with faces parallel to the {111} planes within ± 3°. The lamellas were chemically polished after being cut by spark machining from bigger crystals with a purity better than 99.99%.

The elastic and inelastic intensities at the peaks of the {333} and {444} reflections were measured by using the reflection (Bragg) geometry in the temperature range 295–850 °K. At the scattering angles used in the experiment the crystal samples intercepted all of the incident beam which had a horizontal divergence of 4°. In some cases, the scattered intensities were measured as a function of the angle between the incident beam and the crystal, which was rotated around the goniometer axis. The source and the counter were set at the scattering angle 2θ equal to twice the Bragg angle for the reflection of interest. In many cases, however, the measurements were done only at the maximum of the Bragg peak. Figure 1 illustrates the curves

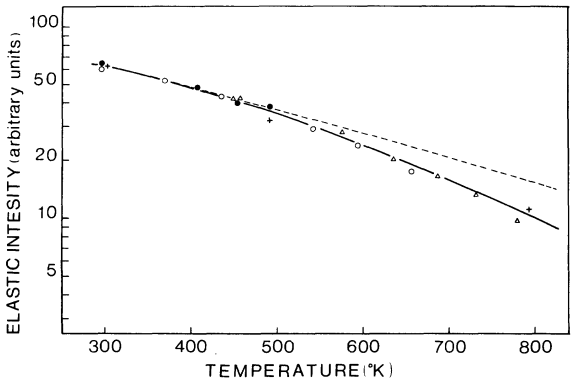

FIG. 2. Temperature dependence of the logarithm of the integrated intensity of the elastic diffraction peak for the {333} reflection. Closed circles, open circles, small triangles, and crosses are experimental points and correspond to measurements taken during different temperature cycles or in different Al samples. The solid line gives the graphical best fit of experimental points. The dashed line gives the temperature dependence in the quasiharmonic approximation which was calculated by taking $\Theta = 395$ °K at room temperature, as explained in the text.

of the scattered intensities versus the angle between the incident beam and the crystal for the {444} reflection at room temperature. The top curve is the intensity I_∞ measured with the source and the absorber out of resonance; the middle one is the intensity I_R, which was measured at resonance. The dashed curve, which has a peak at the Bragg angle, is the intensity of the inelastic scattering and was derived from I_∞ and I_R by applying the formulas (1) of Ref. 4. The base line corresponds to the background of hard γ and cosmic radiations and the straight dashed line corresponds to the 14.4-keV Compton scattering, which was calculated by using a previously reported formula[3] with the values of the incoherent scattering function for Al given by Freeman.[13]

The absolute values of the integrated intensities of the elastic diffraction peaks were obtained by subtracting the area under the inelastic curve from the area under the curve of the total intensity I_∞ and by measuring the intensity of the incident beam attenuated by calibrated Al filters.

The sample was heated by means of a small electric furnace as described in Ref. 5. In order to avoid errors due to incidental bendings of the sample during temperature cycling, the shape of the Bragg peaks was checked and found to be regular at the various temperatures of the experiment.

IV. RESULTS AND DISCUSSION

Elastic Scattering

The absolute values of the integrated intensities of Bragg peaks at room temperature were measured previously and are summarized by Table II of Ref. 4. They were compared with those calculated for both perfect and mosaic crystals. We used the Debye temperature $\Theta = 395$ °K, which is the experimental value for Θ at room temperature as given by Nicklow and Young.[14] The resulting experimental values were very close to those of the mosaic crystal for all reflections investigated ({222}, {400}, {333}, {600}, and {444}). Since the above specimens were used in this work, we may assume the integrated intensities of elastic peaks to be proportional to e^{-2M}, neglecting extinction effects.

The temperature dependences of the logarithm of the integrated intensities are given in Figs. 2 and 3 for {333} and {444} reflections, respectively. The dashed lines in both figures give the temperature dependences calculated by assuming $\Theta = 395$ °K at room temperature and by taking account of the thermal expansion of the lattice as explained by Paskin.[15] In this way, the apparent Debye temperature varies with temperature according to the formula

$$\frac{\Theta_T}{\Theta_{295}} = \left(\frac{1}{1+3\beta(T-295)}\right)^{\gamma}, \tag{10}$$

where β is the linear expansion coefficient and γ is the Grüneisen constant. M was calculated by means of formula (5) corrected by the factor $\Phi(\Theta/T) + \frac{1}{4}(\Theta/T)$, by taking $\gamma = 2.06$, and by taking into account the temperature dependence of β. Both these data were obtained experimentally and are reported in Ref. 16. The above procedure to calculate the temperature dependence of the Debye-Waller factor may reasonably be called the quasiharmonic approximation and was found to agree with the Nickow-Young experiment[14] in the temperature range 78–300 °K. However, as may be seen from both Figs. 2 and 3, the disagreement is evident at

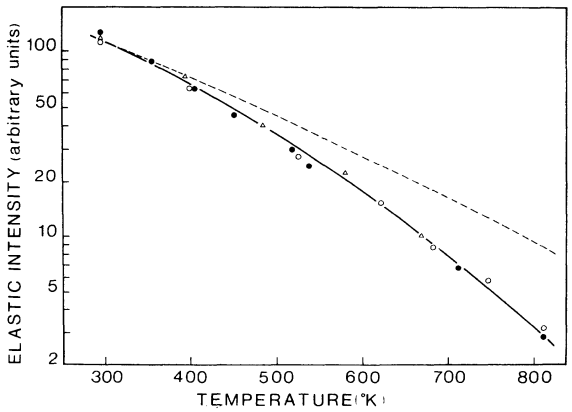

FIG. 3. Temperature dependence of the logarithm of the integrated intensity of the elastic diffraction peak for the {444} reflection. Explanation is as for Fig. 2.

elevated temperatures, suggesting that the amount of anharmonic contributions to the Debye-Waller factor becomes quite considerable with increasing temperature. For example, at 800 °K, at the {444} reflection, the value of $2M$ obtained from experimental data was 4.81, whereas in the quasiharmonic approximation (dashed line) one gets $2M = 3.72$. From the experimental data on Figs. 2 and 3, by taking $\Theta = 395$ °K at room temperature, we obtained two different temperature dependences of Θ for {333} and {444} reflections. These data are reported in Fig. 4 together with those by Nicklow and Young[14] below room temperature, those reported by Chipman[17] from powder-diffraction experiments, and by Dingle and Medlin.[18] As explained in Sec. II, different temperature dependences of Θ for different reflections suggest that the thermal displacements of the lattice atoms do not follow exactly a Gaussian distribution. More precisely, neglecting non-Gaussian terms, it follows from formula (4) that $2M/Q^2$ is independent of the scattering vector $\vec{Q}$, so that the expression

$$\mathfrak{u}(H,H',T,T_0)=\frac{2M_H(T)-2M_H(T_0)}{Q_H^2}-\frac{2M_{H'}(T)-2M_{H'}(T_0)}{Q_{H'}^2}=\frac{Q_H^2-Q_{H'}^2}{12}\left[(\langle u_{iQ}^4\rangle-3\langle u_{iQ}^2\rangle^2)_T-(\langle u_{iQ}^4\rangle-3\langle u_{iQ}^2\rangle^2)_{T_0}\right] \tag{11}$$

is a measure of non-Gaussian anharmonic contributions to the Debye-Waller factor, as was pointed out in Ref. 19. In formula (11), T_0 is a reference temperature and H and H' mean two different reflections $H \equiv \{hkl\}$ and $H' \equiv \{h'k'l'\}$. This argument clarifies the reason why Chipman's data for the {422} reflection and those by Dingle and Medlin for the {511} reflection seem to agree better with those obtained from the {333} reflection than from the {444} one. In fact, $Q_{\{444\}}^2$ is 100% higher than $Q_{\{422\}}^2$, whereas $Q_{\{333\}}^2$ is only 12.5% higher, and finally $Q_{\{511\}}^2 = Q_{\{333\}}^2$.

For mosaic crystals one gets

$$\mathfrak{u}(H,H',T,T_0)=\frac{1}{Q_H^2}\ln\frac{R_H(T_0)}{R_H(T)}-\frac{1}{Q_{H'}^2}\ln\frac{R_{H'}(T_0)}{R_{H'}(T)}\,. \tag{12}$$

Thus information about the amount of non-Gaussian terms can be obtained by measuring the temperature dependences of the integrated intensity $R(T)$ for two different reflections H and H'. Now the non-Gaussian or "anomalous" term

$$\tfrac{1}{12}Q^4(\langle u_{iQ}^4\rangle-3\langle u_{iQ}^2\rangle^2)$$

is proportional to T^3, as was shown in a general way by Maradudin and Flinn.[8] Thus a plot of expression (12) versus $T^3 - T_0^3$ should be linear. This is shown in Fig. 5, where $\mathfrak{u}(\{444\}, \{333\}, T_0, T)$ multiplied by $4\pi^2/a^2$ (a is the lattice parameter) was reported by taking $T_0 = 295$ °K. From the slope of the straight line we obtained

$$\frac{d(\langle u_{iQ}^4\rangle-3\langle u_{iQ}^2\rangle^2)}{dT^3}=1.6\times10^{-44}\ \text{cm}^4\,^\circ\text{K}^{-3}\,.$$

We may compare this result with that calculated by using the expression given by Maradudin and Flinn[8] for a fcc lattice using a nearest-neighbor central-force model. From reflections of the {hhh} type their treatment gives

$$\frac{d(\langle u_{iQ}^4\rangle-3\langle u_{iQ}^2\rangle^2)}{dT^3}=8K_B\left(\frac{1}{3072}\,\frac{\Phi^{(iv)}(\bar{r}_0)}{[\Phi^{(ii)}(\bar{r}_0)]^4}-\frac{1}{4096}\,\frac{[\Phi^{(iii)}(\bar{r}_0)]^2}{[\Phi^{(ii)}(\bar{r}_0)]^5}\right), \tag{13}$$

expressed in terms of the derivatives of the potential energy of interaction $\Phi(\bar{r}_0)$ between nearest neighbors. The $\bar{r}_0$ value is related to the equilibrium value r_0 of the nearest-neighbor separation at temperature T by

$$r_0 = (1+\epsilon)\bar{r}_0\,,$$

where ϵ is the linear expansivity of the lattice. $\Phi(\bar{r}_0)$ is assumed to be a Morse-type potential in

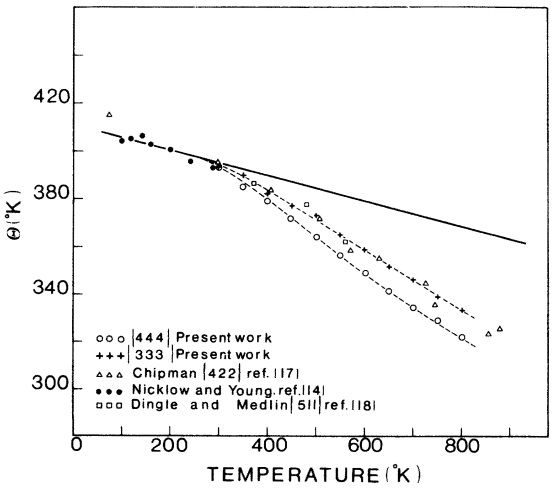

FIG. 4. Different temperature dependences of the x-ray Debye temperature Θ as obtained in the present work and by other authors. The solid line gives the quasiharmonic behavior as calculated by using the Paskin formula (10). Dashed lines show the two different dependences for the {333} and {444} reflections.

order to obtain its fourth derivative

$$\Phi^{(iv)}(\bar{r}_0) = \frac{7}{9}\,\frac{[\Phi^{(iii)}(\bar{r}_0)]^2}{\Phi^{(ii)}(\bar{r}_0)},$$

and use is made of the expressions of ϵ in the high-temperature limit and of the bulk modulus B:

$$\epsilon = -\frac{K_B T}{4\bar{r}_0}\,\frac{\Phi^{(iii)}(\bar{r}_0)}{[\Phi^{(ii)}(\bar{r}_0)]^2}, \quad \beta = \frac{d\epsilon}{dT},$$

$$B = \frac{4}{3\sqrt{2}}\,\frac{\Phi^{(ii)}(\bar{r}_0)}{\bar{r}_0}.$$

By combining all the above formulas, it follows that

$$\frac{d(\langle u_{iQ}^4\rangle - 3\langle u_{iQ}^2\rangle^2)}{dT^3} = 1.095\times10^{-3}\,\frac{\bar{r}_0\beta^2 K_B}{B} = 3.33\times10^{-48}\ \mathrm{cm}^4\,^\circ\mathrm{K}^{-3},$$

which is 4.8×10^3 times lower than the experimental value. However, this disagreement is not surprising since, as was pointed out by Wolfe and Goodman,[11] the method given by Maradudin and Flinn underestimates the contribution of the non-Gaussian term by several orders of magnitude. The two latter authors had to evaluate complicated lattice sums in the reciprocal space, and in order to do that, they made several assumptions, which may have led to fortuitous cancellations between the two terms appearing in expression (13). Moreover, the nearest-neighbor central-force model is not indicated for aluminum, where interactions between the origin atom and atoms in the 8th to 15th shells must be taken into account in order to describe the phonon dispersion curves.[20] By using direct-space sums, Wolfe and Goodman found that the non-Gaussian term in copper was about 10^3 times higher than that calculated by Maradudin and Flinn. Moreover, their method seems to be suitable whatever the interaction-force model one may assume. Thus, it is possible that a better agreement could be achieved between calculated and experimental data also in the case of aluminum crystals.

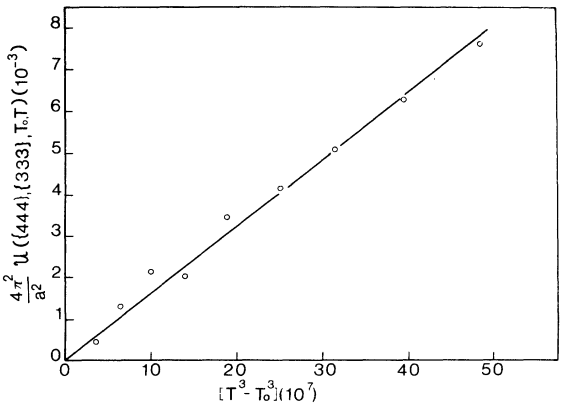

FIG. 5. Plot of $\mathfrak{U}(\{333\}, \{444\}, T_0, T)$ multiplied by $4\pi^2/a^2$ as a function of $T^3 - T_0^3$ ($T_0 = 295$°K). The quantity in the ordinate scale is a measure of the non-Gaussian anharmonic contributions to the Debye–Waller factor (see text).

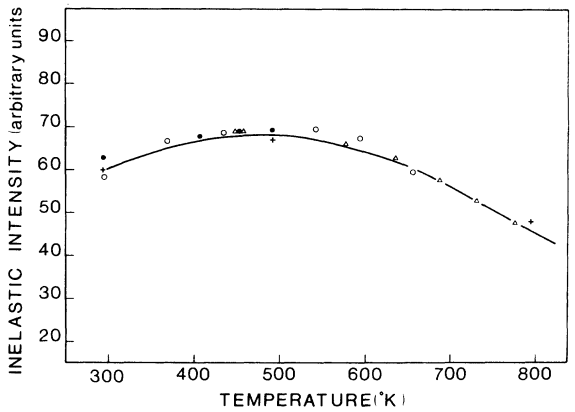

FIG. 6. Temperature dependence of the intensity of the inelastic scattering (TDS plus Compton scattering) at the {333} Bragg peak. The continuous line gives the calculated dependence as explained in the text.

Inelastic Scattering

The temperature dependences of the intensities of the inelastic scattering at the peaks of the {333} and {444} reflections are plotted in Figs. 6 and 7, respectively. In order to compare these results with the calculated temperature dependences of the TDS intensity, it would be necessary to evaluate expression (8) as a function of T and to integrate it over a reciprocal-lattice volume τ determined by the scattering geometry (source and slit sizes and distances; scattering and crystal angles). This

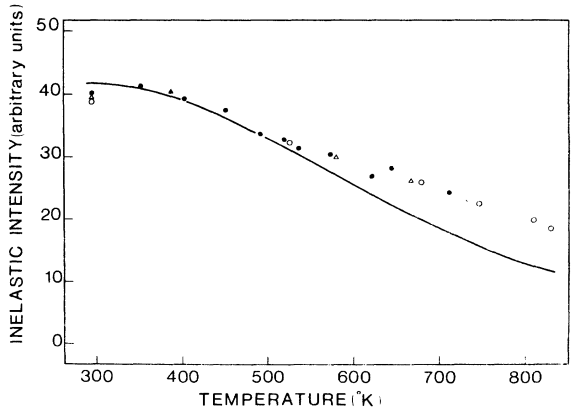

FIG. 7. Explanation is the same as for Fig. 6 except that the experimental point and the calculated curve refer to the inelastic intensity at the {444} reflection.

procedure is difficult to perform, so we tried to calculate the TDS temperature dependence as follows.

The arguments reported in Sec. II suggest that the TDS intensity for a given crystal integrated over τ may be written as

$$R_\tau = e^{-2M} f_\tau(Q, T).$$

In the harmonic approximation the function $f_\tau(T, Q)$ is a sum of several terms: the one-phonon, three-phonon terms, etc., which are proportional, respectively, to T, T^2, T^3, etc. Each of them may be evaluated as a function of the lattice frequencies of the crystal. In order to evaluate R_τ we used the experimental value of e^{-2M} as derived from the measure of the temperature dependence of the elastic intensities, and for $f_\tau(T, Q)$ we used the expression which applies in the harmonic approximation corrected by introducing the temperature dependences of the lattice vibration frequencies.

The procedure which we used to calculate the contribution of the one-phonon term is fully described in Ref. 4, and for the high-order terms we used the approximate methods described in Ref. 5.

The two-phonon contribution was calculated by integrating over τ the expression given by Paskin[21] and by Borie,[22] and the contribution of higher than second-order terms was evaluated by assuming that these terms are constant inside the Brillouin zone.[23] First- and second-order TDS terms were given in Refs. 4 and 5 as a function of the mean velocities v_l and v_t of longitudinal and transverse waves in a polycrystalline sample. Their room-temperature values were taken as $v_l = 6.422 \times 10^5$ cm/sec and $v_t = 3.110 \times 10^5$ cm/sec,[24] and their temperature dependences were assumed to be those

TABLE I. Contributions (in %) of the first-, second-, and higher-order TDS terms and of the Compton scattering to the total inelastic intensity at the {333} and {444} reflections of Al. Different contributions are calculated as explained in the text and in Refs. 4 and 5.

{hkl}	T (°K)	First order	Second order	Higher orders	Compton scattering
{333}	300	88.02	8.81	0.24	2.93
	400	84.92	12.00	0.46	2.62
	500	81.22	15.37	0.84	2.57
	600	77.03	18.78	1.47	2.72
	700	72.43	22.06	2.31	3.07
	800	68.03	25.62	4.08	3.75
{444}	300	78.2	13.93	0.84	6.99
	400	72.64	18.25	1.70	7.41
	500	65.80	22.14	3.24	8.81
	600	57.67	25.00	5.89	11.43
	700	48.08	26.04	10.17	15.71
	800	36.41	24.39	16.87	22.32

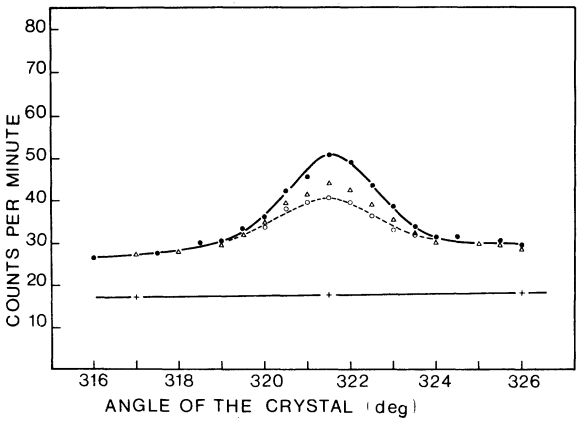

FIG. 8. Scattered intensities vs the glancing angle for the {444} reflection at 700 °K. Explanation is as for Fig. 1.

derived from the phonon dispersion curves in the [310] direction, measured in the range 293–793 °K by means of cold neutron scattering technique.[25] The whole contribution of higher-order terms was expressed as a function of $2M$, whose experimental values are known. Table I summarizes the percentage contribution of first-, second-, and higher-order TDS and of the Compton scattering at various temperatures for both the {333} and {444} reflections. It can be seen that the amount of first- and second-order terms is considerable also at elevated temperature, so that the TDS peak at the {444} Bragg reflection is still well pronounced at 700 °K as is shown in Fig. 8. Previously reported[4] room-temperature measurements of the TDS intensity at several reflections in Al were found to have a dependence on $\sin\theta/\lambda$ in agreement with that of the one-phonon term. However, this does not contradict the present work since it is found that the correction for the multiphonon terms does not alter considerably the $\sin\theta/\lambda$ dependence in Al. For example, the ratio of the TDS intensities at the {333} and {444} reflections is changed by about 6%, so that the precision of the measurements reported in Fig. 8 of Ref. 4 makes it impossible to evidence the effect of the multiphonon correction.

The calculated dependences of the inelastic scattering intensities (TDS plus Compton scattering) are given by the continuous lines in Figs. 6 and 7. The agreement with experimental data is good for the {333} reflection, whereas the calculated temperature dependence is appreciably faster than the experimental one in the case of the {444} reflection. The argument that this discrepancy may be due to an erroneous evaluation of the amount of the Compton scattering is scarcely reliable. In fact, the Compton intensity should be increased by a factor 5.6 in order to fit the experimental data of

the {444} reflection. This factor is considerably higher than the uncertainty derived by using the formula reported in Ref. 3 (for example, the evaluation of the reciprocal-lattice volume τ); moreover, the arbitrary assumption of a factor 5.6 would cause a 10% discrepancy between the calculated and experimental temperature dependence for the {333} reflection. It is also worthwhile to remember here that the entire above-mentioned method for calculating the several-order TDS contributions and the Compton scattering resulted in good agreement with experiment both for Si and for KCl crystals, where the one-phonon term and the high-order terms predominate, respectively. For the KCl crystals there was evidence that the harmonic or the quasiharmonic approximation was sufficient to explain the temperature dependence of the Debye–Waller factor. Since for aluminum the contrary happens, we advance the hypothesis that the observed deviations in the temperature dependence of the inelastic intensity at the {444} Bragg peak are due to anharmonic contributions to the TDS intensity. By introducing in the above calculation the experimental values of $2M$ and the temperature dependence of the lattice frequencies these contributions are not taken into account.

Comparing formulas (7) and (8) of Sec. II and having in mind the standard procedure for calculating the TDS intensity,[1] we observe that the function $f_\tau(Q, T)$ can be written by means of a sum of increasing-order TDS terms only if non-Gaussian contributions are unimportant. But the presence of the term $Q^4\mathfrak{F}$ in the argument of the exponential in formula (8) introduces additional complications which should become more and more important with increasing Q. For example, if the presence of the term $Q^4\mathfrak{F}$ becomes important at about 550 °K at the {444} reflection (see Fig. 7), the corresponding temperature for the {333} reflection would be 810 or 980 °K if $\mathfrak{F}$ is proportional to T^3 or T^2, respectively. Now, $\mathfrak{F}$ will be a sum of terms proportional to T^2 and T^3. The fact that we observe a disagreement for the {444} and not for the {333} reflection is not surprising, if we consider that the explored temperature range extends only to about 800 °K.

V. CONCLUSIONS

The Mössbauer effect was used to separate the elastic and inelastic parts of the scattered intensities at the {333} and {444} Bragg reflections in Al crystals in the temperature range 295–800 °K. The most significant results are the following.

(a) The temperature dependences of the integrated intensities of elastic peaks show large anharmonic contributions to the Debye–Waller factors. By analyzing these results in light of the existing theory of the effect of anharmonic interactions on the x-ray-scattered intensities, it was proved that effects coming from deviations from a Gaussian distribution of the thermal displacements of the atoms are detectable in aluminum. The non-Gaussian contribution to the Debye–Waller factor was found to be about 10^3 times larger than that estimated by means of the approximated method of Maradudin and Flinn[8] for a nearest-neighbor central-force model. More sophisticated methods like those used by Wolfe and Goodman[11] should give more correct results.

(b) Some discrepancies between experimental and calculated temperature dependences of the inelastic intensity at the {444} reflection were observed. By comparing this result with previous results on Si and KCl crystals, the above discrepancies were interpreted as due to anharmonic contributions to the TDS intensity. Such contributions are over and above those due to the introduction in the calculations of the experimental values of the Debye–Waller factor and the temperature dependence of the lattice frequencies.

Finally, we advance the hypothesis that the role of non-Gaussian terms in the correlation part of the TDS intensity may be important.

[1]B. E. Warren, *X-Ray Diffraction* (Addison-Wesley, Reading, Mass., 1969), Chaps. 3–11.
[2]I. Waller, Ann. Phys. (Leipz.) **83**, 153 (1927).
[3]C. Ghezzi, A. Merlini, and S. Pace, Nuovo Cimento B **64**, 103 (1969).
[4]G. Albanese, C. Ghezzi, A. Merlini, and S. Pace, Phys. Rev. B **5**, 1746 (1972).
[5]G. Albanese, C. Ghezzi, and A. Merlini, Phys. Rev. B (to be published).
[6]M. A. Krivoglaz and F. A. Tekhonova, Kristallografiya **6**, 496 (1961) [Sov. Phys.-Crystallogr. **6**, 399 (1961)].
[7]H. Hahn and W. Ludwig, Z. Phys. **161**, 404 (1961).
[8]A. A. Maradudin and P. A. Flinn, Phys. Rev. **129**, 2529 (1963).
[9]Y. Kashiwase, J. Phys. Soc. Jap. **30**, 320 (1965).
[10]B. T. M. Willis, Acta Crystallogr. A **25**, 277 (1969).
[11]G. A. Wolfe and B. Goodman, Phys. Rev. **178**, 1171 (1969).
[12]A. Guinier, *Théorie et Technique de la Radiocristallographie* (Dunod, Paris, 1956), Chap. XIII, p. 497.
[13]A. J. Freeman, Phys. Rev. **113**, 176 (1959).
[14]R. M. Nicklow and R. A. Young, Phys. Rev. **152**, 591 (1966).
[15]A. Paskin, Acta Crystallogr. **12**, 929 (1959).
[16]R. M. Nicklow and R. A. Young, Phys. Rev. **129**, 1936 (1963).
[17]D. R. Chipman, J. Appl. Phys. **31**, 2012 (1960).
[18]R. E. Dingle and E. H. Medlin, Acta Crystallogr. A **28**, 22 (1972).
[19]N. M. Butt and G. Solt, Acta Crystallogr. A **27**, 238 (1971).
[20]J. L. Yarnell and J. L. Warren, in *Lattice Dynamics*, edited by R. F. Wallis (Pergamon, New York, 1965).
[21]A. Paskin, Acta Crystallogr. **11**, 165 (1958).

[22]B. Borie, Acta Crystallogr. **14**, 566 (1961).
[23]This latter assumption was proved to be consistent in KCl by showing that at sufficiently high temperatures, when the higher-order terms predominate, the TDS intensity has no more peaks at the Bragg angle (see Ref. 5).
[24]R. E. Schmunk and C. S. Smith, J. Phys. Chem. Solids **9**, 200 (1959).
[25]K. E. Larsson, N. Dahlborg, and S. Holmryd, Ark. Fys. **17**, 369 (1960).

PHYSICAL REVIEW B VOLUME 8, NUMBER 4 15 AUGUST 1973

Structures and a Two-Band Model for the System $V_{1-x}Cr_xO_2$†

J. B. Goodenough and H. Y-P. Hong
Lincoln Laboratory, Massachusetts Institute of Technology, Lexington, Massachusetts 02173
(Received 25 September 1972)

The evolution with x of the monoclinic-to-tetragonal transition temperature and of the room-temperature monoclinic structures of the system $V_{1-x}Cr_xO_2$ have been reexamined and extended to cover the entire solid-solution range $0 \leq x < 0.20$. The space group of the room-temperature monoclinic phase changes from $P2_1/c$ at $x = 0$ to $C2/m$ for $0.005 \leq x \leq 0.065$ and $P2/m$ for $0.07 \leq x < 0.20$. The monoclinic $P2/m$ structure is determined for the first time. The distortion from tetragonal symmetry is accomplished by a contraction of the V-O bonds in the tetragonal $(110)_r$ planes and an expansion in the $(1\bar{1}0)_r$ planes. The structures and the conductivity changes are interpreted in terms of two overlapping bands that change their relative stabilities with x. The substitutional Cr^{3+} ions, which have a localized-electron d^3 configuration, also perturb the electron potential sufficiently to induce, at larger x, a $3d$-electron localization on the vanadium ions.

INTRODUCTION

Stoichiometric VO_2 exhibits a first-order semiconductor-to-metal transition at $T_t = 340$ K. The metallic high-temperature phase has the tetragonal ($P4_2/mnm$) structure of rutile, and the low-temperature phase is monoclinic ($P2_1/c$). The relationship of these two phases to one another is illustrated in Fig. 1. In the rutile structure, V^{4+}-occupied octahedra form edge-shared strings parallel to the tetragonal c_r axis. In the low-temperature phase, these strings are broken up into V-V pairs, the uniform cation separation of 2.88 Å within a string disproportionating into 2.62 Å within a V-V pair and 3.16 Å between pairs.[1] In addition, the axis of each pair is tilted away from the c_r axis to make a shortest V-O separation of 1.76 Å. The bridging anions of a pair have V-O separations of 1.86 and 1.89 Å.[2] There is no magnetic order in the low-temperature phase.[3]

The low-temperature structure is suggestive of homopolar V-V bonding, as was already pointed out by Magnéli,[1] and Goodenough[4] anticipated the lack of magnetic order by pointing out that homopolar bonding could also account for the semiconductor-to-metal transition.

From the symmetry constraints of the structures and known trends in the physical properties of transition-metal oxides, it is also possible to identify the essential features of the energy diagrams for these two phases.[5,6] In vanadium oxides, the Fermi energy E_F falls above the top of the O^{2-} $2p$ band and below the vanadium $4s$ band. Therefore, formal valences can be used to designate the number of d-like electrons present per vanadium ion. Orthorhombic crystalline fields split the d^1 energies at the V^{4+} ions into two unstable σ-bonding orbitals, two quasidegenerate π-bonding orbitals, and a stable $d_{\parallel}$ orbital oriented along the c_r axis of the tetragonal cell. A critical V^{4+}-V^{4+} separation $R_c = 2.94$ Å has been estimated for the transition from itinerant to localized behavior of the $3d^1$ manifold in oxides containing a V^{4+}-ion subarray.[7] Therefore, the $3d$ orbitals parallel to the c_r axis should form a narrow $d_{\parallel}$ band in tetragonal VO_2 (see Fig. 2). From data for the transition-metal oxides with perovskite structure, it is known that covalent mixing between oxygen $2p$, both p_π and p_σ, and the V^{4+}-ion $3d$ orbitals is strong enough to create itinerant-electron d-like orbitals.[6,8] Therefore, the two σ-bonding d orbitals per V^{4+} ion form unstable σ^* bands and the two π-bonding d orbitals form quasidegenerate π^* bands via V^{4+}-O^{2-}-V^{4+} interactions. Observation[9] of a nearly isotropic conductivity in single-crystal VO_2 was interpreted[6] to indicate that the π^* bands overlap the Fermi energy E_F.

In the monoclinic phase, V-V pairing along the c_r axis splits in two the narrow $d_{\parallel}$ band (which may already be split in the tetragonal phase by electron correlations). The semiconducting character of the monoclinic phase requires that the π^* bands be raised above E_F and that the formation of V-V pairs stabilize V-V homopolar-bond orbitals below E_F, as shown in Fig. 3. Since 2.62 Å $< R_c$ and 3.16 Å $> R_c$, it follows that in the monoclinic phase